Analytical Methods

Cite this: *Anal. Methods*, 2012, **4**, 2381

www.rsc.org/methods

PAPER

Electrochemical aging of silver nanoparticles and its effects on bio-chemical sensing properties

Jun Liu, Penglan Chai, Jun Tang,* Huanfei Wen, Yunbo Shi and Chenyang Xue

Received 15th November 2011, Accepted 30th April 2012
DOI: 10.1039/c2ay05786g

In this work, interesting findings on the change in time stability for SERS and SEF based bio-chemical sensing properties of Ag nanoparticle films are reported. Ag nanoparticles were deposited on a Si or SiO_2 substrate using DC magnetron sputtering. By immersion of the Ag nanoparticle films into the Crystal Violet (CV) aqueous solutions, the long time stability of Ag nanoparticle films, from both the morphology, and SERS and SEF based sensing performances, were measured. Some key parameters like CV concentration and substrate conductivity were also discussed. We believe that the results reported in this paper can provide us with a reference regarding the environmental stability of the metal nanomaterials as well as their precision or reliability in the development of highly sensitive bio-chemical sensors.

1 Introduction

As a multifunctional material, Ag nanoparticles were widely applied in catalysis, optics, electronics and other areas, due to their unique size-dependent optical, electrical and magnetic properties. Using the surface plasmon polariton resonances (SPPR) excited by electromagnetic (EM) radiation, Ag nanoparticles have already been applied as the sensing probes of the highly sensitive bio-chemical sensors. Surface enhanced fluorescence (SEF) and surface enhanced Raman scattering are two popular techniques for detecting micro-quantities of biomolecules. From reports in previous literature, it has been concluded that, of the three noble metals that display plasmon resonances, Ag exhibits the highest efficiency of plasmon excitation, which makes it one promising material for bio-chemical sensing applications.[1–3]

In order to be commercially practical, all the bio-chemical sensing materials must be stable over long periods of time. This is always a key issue for the design of the sensors. Unlike bulk metal, Ag nanoparticles are much more active to the atmospheric environment, which is depended on their sizes, density and patterns.[4,5]

In one hand, the special properties of Ag nanoparticles has already been demonstrated and applied for the self-assembly of Ag nanomaterials into well organized nanostructures, which further expand their applications of the Ag nanoparticles in fields like catalysis, nanophotonics *etc.* From our previous research, we have already found that Ag nanoparticles are quite sensitive to environmental materials. Using this knowledge, we have developed a novel plasma-induced 2-dimensional Ag nanoparticle self-assembly process, due to the Ostwald ripening effect.[6,7] The proposed process provides a rapid method of tailoring the nanoparticle size, density, and shape distribution, is amenable to large-scale production, and compatible with the fabrication of solar cells and biosensors.[8]

The Ag nanostructure fabrication, or self-assembly process, has also been widely studied. Kim and his colleagues reported a one-pot fabrication of silver nanostructures on substrates using electron beam irradiation.[9] Through a simple alteration of electron beam conditions, silver nanomaterials of different sizes and shapes were fabricated, such as nanocubes, nanorods, nanoparticles and nanonetworks. Tang *et al.* has reported two dimensional (2D) fractal structures formed from fairly uniform Ag island films on insulating silicon dioxide surfaces upon immersion in deionized water.[10] This result is distinctly different from the previously observed three-dimensional (3D) growth of faceted Ag nanocrystals on conductive surfaces (ITO and graphite).

On the other hand, it can also be concluded from the literature that the morphology changes of the Ag nanostructures after environmental exposure can also change their optical properties or bio-chemical sensing performances. Rowlen's group has reported a study on the effect of solvent exposure on thin Ag film optical properties and their surface morphologies.[11] They found that when thin Ag films were dipped in a solvent, a common method for analyte application, the optical extinction spectra contained a blue-shift of more than 20 nm with a significant reduction in optical density. Over a time period of 60 min, the optical spectra gradually shifted back toward the original pre-dipped profiles, but did not return completely to normal. Miller *et al.* have recently studied the aging induced Ag nanoparticle

Key Laboratory of Instrumentation Science & Dynamic Measurement, Science and Technology on Electronic Test & Measurement Laboratory, North University of China, Taiyuan, Shanxi, China. E-mail: tangjun@nuc.edu.cn

rearrangement under ambient atmosphere and consequences for nanoparticle-enhanced DNA bio-sensing.[12] The effect can be observed with an exposure time as short as two days, and a nearly 17-fold signal enhancement can be achieved after 30 days of aging. Redmond *et al.* reported processing silver nanoparticles electrochemically OR in water,[13] where silver nanoparticles were thermally evaporated on conducting substrates spontaneously and evolved in size when immersed in pure water. The researchers demonstrated the sensitivity of the electrochemical properties of metallic nanostructures at remarkably large sizes around 50 nm. They believe that this result will affect bare metallic nanostructures on conducting substrates even in the absence of water. Gentry *et al.* studied the factors that control Ostwald ripening in a bimodal silver nanocolloid system containing tabular particles having one dimension equal to or less than 5 nm. This gives us an insight into the colloid stability working in the nanotechnology regime.[14]

In conclusion, Ag nanomaterial was widely used in fields such as bio-chemical sensing, catalysis, nanophotonics *etc.* Due to its sensitivity to external environments such as plasma,[8,15] electron beams,[9] oxygen[16,17] and water among other substances,[18–21] different silver nanostructure fabrication or self-assembly processes were developed. This behavior has also caused the instability of the Ag nanostructures, both from the morphology and optical properties. However, from the reported literature, the time stability of the Ag nanostructures when exposed to the external environment is still unclear, especially in one of the most researched fields; highly sensitive bio-chemical sensing using Surface Enhanced Raman Spectroscopy (SERS) and Surface Enhanced Fluorescence (SEF).

In this paper, we report an interesting finding on the time stability of the SERS and SEF properties of Ag nanoparticle films. Using DC magnetron sputtering, Ag nanoparticle films were deposited on P-doped silicon or thermal SiO_2 substrate was deposited on silicon wafers. Crystal Violet (CV) diluted in water was used as the validating chemical solution for the test. By immersion of the Ag nanoparticle films into the CV diluted in water, the SERS and SEF of the nanoparticle films' long-standing stability to the chemical molecules were measured. To understand the spectroscopy evolution of the Ag nanoparticle films in the CV solution with different treatment times, the time stability for the morphology of the Ag nanoparticle films was also characterized using AFM. Some key parameters like CV concentration and substrate conductivity were also discussed. We believe that the results reported in this paper can provide us with a reference for the environmental stability of the metal nanomaterials and their effects on the precision and reliability when developing highly sensitive bio-chemical sensors.

2 Experimental

Ag nanoparticles were deposited using DC sputtering (JTRC-550, China). Since the Ag sputtering target can be easily polluted in air due to the chemical reactions of Ag with air, before nanoparticle deposition, a surface cleansing process was always performed by sputtering with a low Ar flow rate of about 10 sccm for 5 min. Polished P-type silicon wafers and P-type silicon wafers with 1 μm thermal SiO_2 were used as the substrate materials. The Ag nanoparticle depositions were performed under room temperature for 2 min in our experiment.

The SERS and SEF characterizations were performed after immersion of the samples into a solution of CV aqueous solutions and dried prior to the acquisition of the spectra. Different immersion times and solution concentrations were used to test the parameters affecting nanoparticle aging. The samples were excited using a 514.5 nm laser line from the Renishaw Raman Microscope System Invia. For this series of measurements, an excitation power beam of 5 mW was used in order to minimize heating and photo-bleaching effects.

Nanoparticle topography characterization studies were performed with an Atomic Force Microscope (AFM, CSPM-3400, China). The AFM measurement results presented in this paper were recorded under tapping mode. The nanoparticle sizes and density calculations were performed with the assistance of IMAGER (Ver. 4.60). Due to the lateral enlargement of the AFM measurements for the nanoparticles, the diameters of the nanoparticles calculated in this paper were mainly from the heights of the nanoparticles.

3 Results and discussion

3.1 Time dependence of Ag nanoparticle ripening process

To have a systematical understanding of the nanoparticle aging process under given chemical solutions, and the potential effects of nanoparticle aging on bio-chemical sensing performances, both the photoluminescence (PL) and the Raman spectra of the CV on Ag nanoparticle films were measured. The freshly prepared Ag nanoparticle films on SiO_2 substrate (with the resistivity of about 10^2 to 10^3 Ω cm) were immersed into the CV solutions with a concentration of 10^{-5} mol L^{-1} diluted in water. Different immersion times were used to study the effects of aging: 0 hours, 1 hour, 7 hours, 72 hours (3 days), 168 hours (1 week), 240 hours (10 days), and 336 hours (2 weeks). All the samples with different immersion times were taken out of solution and air-dried. The PL and Raman measurements were performed immediately after the solution was dried on the sample surface.

Fig. 1(a) and (c) display the Raman and PL spectra of the CV on the Ag nanoparticle films with different aging times. From the calculated intensity variations of the Raman and PL spectra, it can be concluded that, with the aging of silver nanoparticles, there is a clear decrease of both Raman and PL intensity as is shown in Fig. 1(b) and (d). For the PL spectrum, the intensity was decreased from 13 082 ± 671 (a.u.) to 379 ± 24 (a.u.) after 2 weeks of immersion in the CV solution, corresponding to a 34.5 fold decrease in intensity. Meanwhile, for the Raman intensity, such as the Raman peak of 1588 cm^{-1} (ref. 22 and 23), the intensity was decreased from 101 750 ± 3761 (a.u.) to 2143.6901 ± 71 (a.u.) after 2 weeks of immersion, which is a 47.5 fold of variation. Also, a continuous decrease in both Raman and PL intensities was observed, which began at a higher decreasing speed and then gradually stabilized.

In order to understand the mechanism behind these spectra variations, the structural characterization of the nanoparticle aging effects were performed using AFM, as shown in Fig. 2(a)–(g). From the calculation results of the AFM measurements, and as we can see in the insets of the images, we can easily calculate the

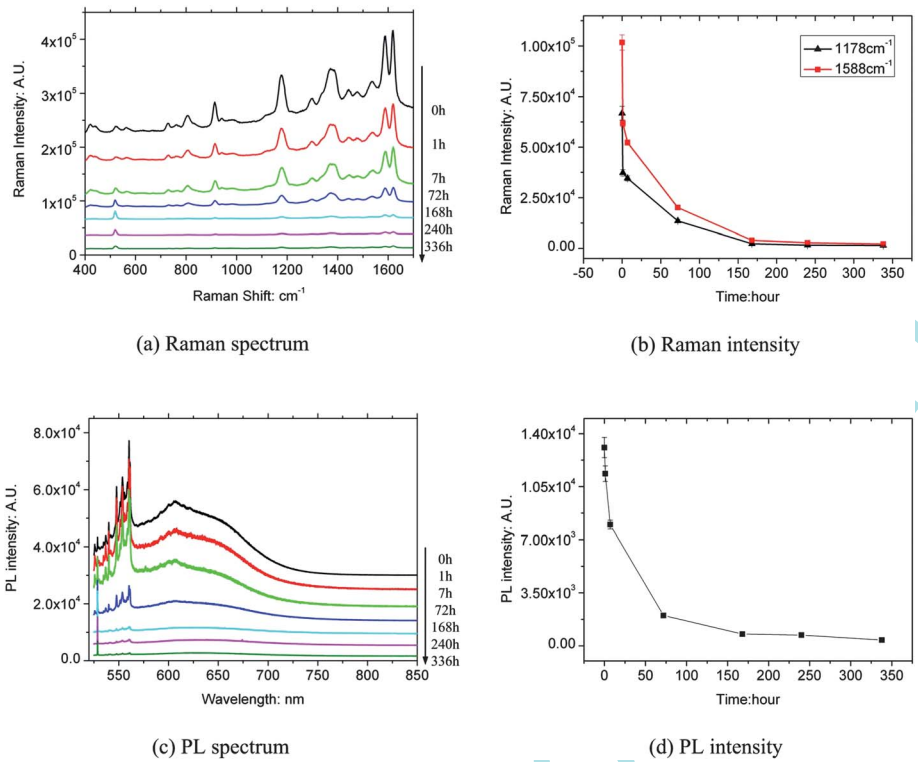

Fig. 1 Raman and PL spectra of the Ag nanoparticle films (on SiO_2 substrate) evolution with different immersion time in the 10^{-5} mol l^{-1} CV aqueous solutions.

nanoparticle size distribution and density changes. For a 2 min deposition, the prepared Ag nanoparticle film has a mean diameter of 5.58 ± 1.1 nm and a density of about 1.16×10^{11} cm^{-2}.

As the samples remained in the CV solution for longer periods of time, the nanoparticle sizes were seen to increase quite fast in the beginning, and after 7 hours of immersion, we saw a shift as sizes at increasing speed started to become smaller and smaller.

We have further calculated the sizes and density evolution of the nanoparticle films, as is shown in Fig. 2(h). From these results, we conclude that compared with the prepared samples, the increase of the nanoparticle sizes from 5.58 ± 1.1 nm to 7.92 ± 0.02 nm and the decrease of the nanoparticle density from 1.16×10^{11} cm^{-2} to 5.68×10^{10} cm^{-2} occurred quickly. These results were seen within the first 7 hours immersion of the samples in the solution. Both the speed of nanoparticle sizes and density variations were quite small from 7 hours of immersion until two weeks (336 hours) of immersion. After two weeks the nanoparticle sizes and density began to stabilize. From all these processes, variations in nanoparticle mean diameters were observed to be about 2.3 times greater and variations in density were found to be about 5.2 times less.

The observed nanoparticle size and density evolutions can be explained using the OR process which is observed in solid (or liquid) solutions and describes the evolution of a non-homogenous structure over time.[24,25] It is a process that depends on both the physical chemistry of the compound and the particle size distribution. The ripening process of the SiO_2-supported Ag nanoparticles can be described as follows:[11,13,18] when Ag nanoparticles with a broad size distribution on a conductive substrate are immersed in water, the smaller nanoparticles dissolve, producing Ag^+ ions in the water and electrons in the conductive substrate. The ions diffuse through the water from small to large particles while the electrons travel through the substrate. The net effect is for the smaller particles to disappear and the larger particles to grow even larger, and thus, this process is called electrochemical Ostwald ripening.

Another mechanism can be used to explain the morphology variations of these nanoparticle films; the so-called 'kinetic Diffusion Limited Aggregation (DLA) model' proposed by Roark and Li.[11,26] The process starts with a seedling structure or nucleation site, normally a single point, and the cluster growth involves particle diffusion until it sticks irreversibly and becomes part of the structure.

This dynamic process of the nanoparticle film was first described numerically by J. Warren and B. Murray using the phase-field model,[25] which can give us some insight into the experimental results we obtained. Warren *et al.* have simulated the evolution of the concentration patterns for two computations of 200 drops on a 500×500 grid with initial volume fractions of 10% and 20% respectively. From the simulation results, it was concluded that during the Ripening process, after a precipitous decrease in nanoparticle density and a rapid rise in nanoparticle size early on, the system settles down into a more regular coarsening regime. This theoretical conclusion is similar to that regarding our nanoparticle size and density evolution at the beginning. There was a noticeably fast increasing of nanoparticle diameters and noticeably fast decreasing of the density within the first 7 hours. This trend was gradually stabilized until after 336 hours' treatment.

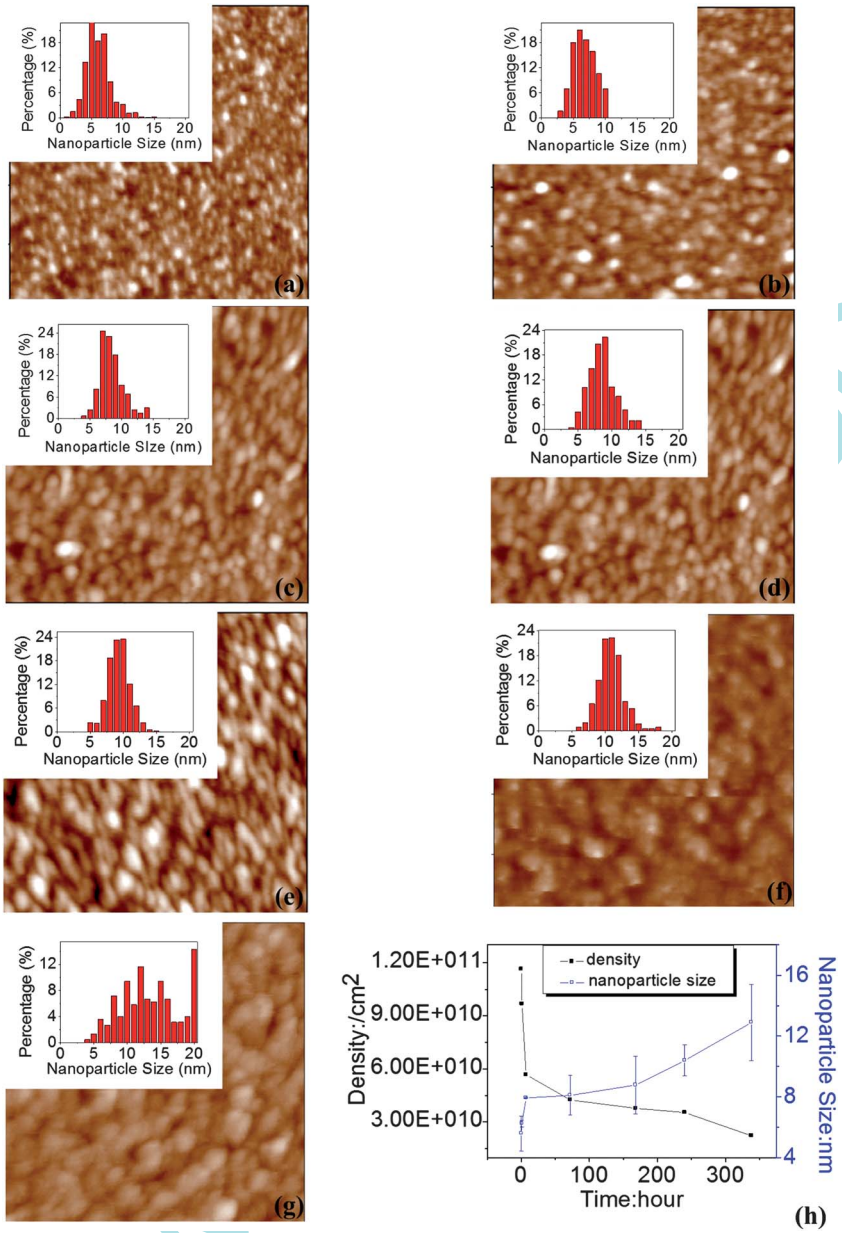

Fig. 2 AFM images of the Ag nanoparticle size and density evolution with time: (a) 0 hour, (b) 1 hour, (c) 7 hours, (d) 72 hours, (e) 168 hours, (f) 240 hours, (g) 336 hours, (h) data conclusion.

3.2 Different substrates

Next, we investigated the effect of substrates on Ag nanoparticle aging under chemical solutions. P-doped silicon (with a resistivity of about 7 to 12 Ω cm) was used as the substrate. With the same experimental conditions, we deposited the Ag nanoparticles for 2 min. The Raman and PL spectra were recorded and the intensity variations were concluded as is shown in Fig. 3. From these results, it can be concluded that, with the silicon substrate, both the Raman and PL intensities were much weaker, compared with the SiO_2 substrate spectra. Also, the variations in intensity were much smaller, with 2.94 fold and 10.7 fold variations for Raman and PL methods respectively. Another difference observed on the silicon substrate was that both the Raman and PL spectra had an increase in intensity after 72 hours of immersion in CV solution. After 72 hours, both decreased.

The variations in Raman and PL spectra intensities can also be understood from the nanoparticle film morphology evolutions. Using the same method, the Ag nanoparticle sizes and densities were calculated, as is shown in Fig. 4. From the measurement results, it can be concluded that there was a quite fast increase in nanoparticle size, from 6.13 ± 0.2 nm at the beginning to 22.2 ± 3.89 nm when measured after 72 hours of immersion in the CV solution. In summary this was a 3.6 fold increase. Simultaneously, the nanoparticle density decreased from 9.75×10^{10} cm^{-2} to 2.19×10^{10} cm^{-2} within 72 hours of treatment. Eventually the nanoparticle density and size variation became much weaker and gradually stabilized.

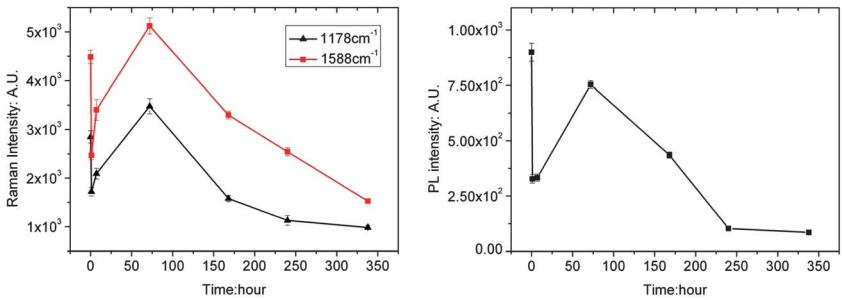

(a) Raman intensity (b) PL intensity

Fig. 3 Raman and PL spectrum of the Ag nanoparticle films (on Si substrate) evolution with different immersion time in the 10^{-5} mol l^{-1} CV aqueous solutions.

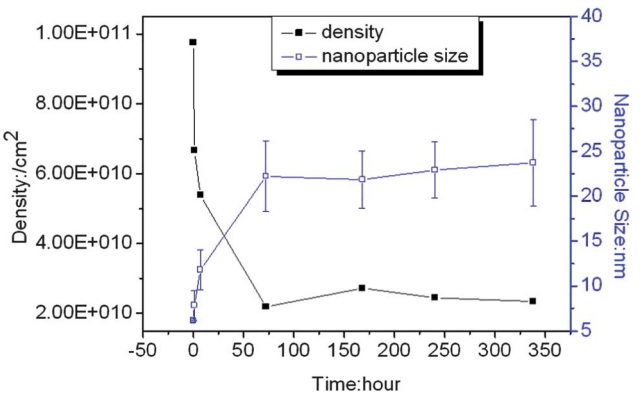

Fig. 4 AFM measurement results of the Ag nanoparticle size and density evolution with time.

From the nanoparticle morphology evolution, a much faster ripening process was observed on the silicon substrate, in comparison with the morphology evolution on the SiO_2 substrate. This ripening process of the Ag nanoparticles was assisted by the conductive Si substrate, which created a much more rapid flux in nanoparticle density and size in the first 7 hours. Additionally, the speed of the ripening process was saturated much faster than what we observed on the SiO_2 surface.

This ripening process can be described by two process as we have also demonstrated before:[8,16] intercluster transportation by either surface diffusion driven by capillary forces along the substrate, or vapor phase transportation along the atmosphere. The Ag ion plates out onto the larger nanoparticle by accepting an electron and accepting an electron from a neighboring smaller particle through the substrate.[13] We believe that, due to the higher electron mobility, the ripening speed of the nanoparticles on Si substrate is much faster and bigger, which is quite evident as we observed in the first 7 hours.

3.3 Different concentrations

In the following experiment, the CV solution concentration was also investigated as a parameter affecting the Ag nanoparticle aging process. We kept the other experimental parameters constant except the CV concentration which was changed to 10^{-4} mol L^{-1}. Ag nanoparticles deposited on SiO_2 substrate surfaces were used in this study. From the intensity variations of the PL and Raman spectra, as shown in Fig. 5, it can be concluded that, with the aging of silver nanoparticles, both Raman and PL intensities remained similar within the first 7 hours of treatment. But after the first 7 hours, a clear decrease in both PL and Raman intensity was observed. For the PL spectrum, the intensity was decreased from 7576 ± 421.4 (a.u.) in the beginning to 2004 ± 301 (a.u.) after 2 weeks of immersion in the CV solution, corresponding to a 3.78 fold of decreasing intensity. Meanwhile, for the Raman intensity, such as the peak of 1588 cm^{-1}, the intensity was decreased from 77 192 ± 2185 (a.u.) in the beginning to 17 392 ± 537 (a.u.) after 2 weeks of immersion, which we calculated as a 4.4 fold variation. A continuous decrease of both Raman and PL intensities was observed.

The effect of the pH value of the acidic solution to the ripening process of Ag nanoparticles has already been reported. Previous studies have found that acidic solutions can speed the ripening process. The Ag nanoparticles can be dissolved in water, but this is dependent on the pH value of the solution:[13]

$$4Ag + O_2 + 4H^+ \rightarrow 4Ag^+ + 2H_2O$$

Meanwhile, the existence of the Cl^- ions from the CV in the aqueous solutions can also react with the Ag^+ ions:

$$Ag^+ + Cl^- \rightarrow AgCl$$

In this experiment, by increasing the concentration of the CV in aqueous solution, the Cl^- ions were also increased, which increased the speed of the ripening process. As is shown in Fig. 6, within the first 7 hours of immersion, there was a rapid increase of the nanoparticle size, from 3.49 ± 2.1 nm to 21.8 ± 3.4 nm, and a rapid decrease in nanoparticle density, from 2.29×10^{11} cm^{-2} to 2.36×10^{10} cm^{-2}. After 7 hours of immersion, a clear decrease in nanoparticle size was observed, with a reduction of 9.45 ± 1.54 nm.

We believe that this is due to the higher concentration of CV in the aqueous solutions, which lead to a higher Cl^- ion concentration. After a long period of immersion, more and more Ag^+ reacted with the Cl^- ions, forming AgCl dissolved in solution, which reduced the quantity of Ag on the substrate. Thus, in this experiment, a clear decrease in the nanoparticle size was observed after 7 hours of immersion in the 10^{-4} mol l^{-1} CV solutions.

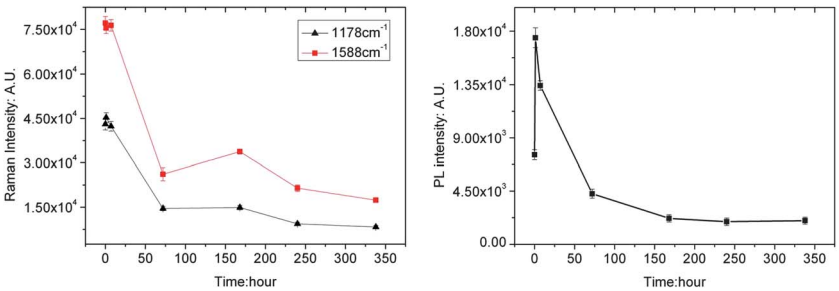

(a) Raman intensity (b) PL intensity

Fig. 5 Raman and PL spectrum of the Ag nanoparticle films (SiO_2 substrate) evolution with different immersion time in the 10^{-4} mol l^{-1} CV aqueous solutions.

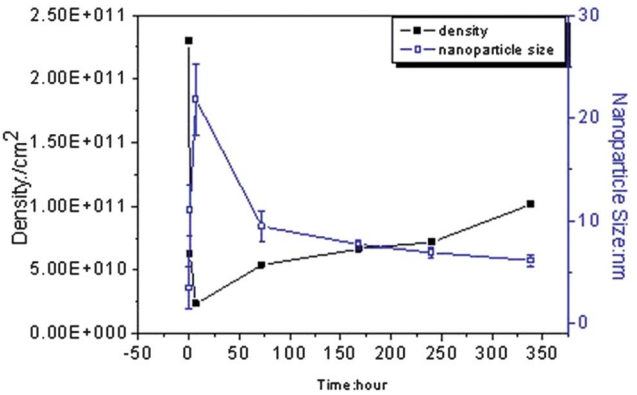

Fig. 6 AFM measurement results of the Ag nanoparticle size and density evolution with time.

4 Conclusions

In conclusion, the stability over time of the SERS and SEF properties of the Ag nanoparticle films were reported in this paper. Crystal Violet (CV) diluted in water was used as the validating chemical solution for the test. By changing the immersion time of the Ag nanoparticle films in the CV solutions, a clear change in both Raman and PL intensities was observed. The change in intensity was found to be a 47.5 fold decrease in Raman intensity and a 34.5 fold decrease in PL intensity after two weeks of aging in CV aqueous solutions.

The AFM measurement results of these Ag nanoparticle films helped us to understand the mechanism of these PL and Raman spectra variations. A clear increase of the nanoparticle size and decrease in nanoparticle density were seen, which were mainly caused by the CV solution assisted Ripening of the nanoparticle films. By changing the substrate conductivity and the concentration of the chemical solutions, the aging effect of the Ag nanoparticle film was also altered. From the morphology point of view, better conductivity and higher concentration of the chemical solution will lead to a stronger change in nanoparticle size and density. This behavior usually happened much faster in the first few hours. Although the mechanism of this phenomenon is still unclear, we believe that the results reported in this paper can provide us with a reference for the stability of metal nanomaterials exposed to bio-chemical solutions which could prove to be of critical importance when developing highly sensitive bio-chemical sensors.

Acknowledgements

This project is supported by the National Nature Science Foundation of China (91123016, 51105345), Nature Science Foundation of Shanxi Province (2011021016), Shanxi Scholarship Council of China (2011068).

References

1 S. Morton, D. Silverstein and L. Jensen, Theoretical studies of plasmonics using electronic structure methods, *Chem. Rev.*, 2011, **111**, 3962–3994.
2 K. Mayer and J. Hafner, Localized surface plasmon resonance sensors, *Chem. Rev.*, 2011, **111**, 3828–3857.
3 M. Stewart, C. Anderton, L. Thompson, J. Maria, S. Gray, J. Rogers and R. Nuzzo, Nanostructured plasmonic sensors, *Chem. Rev.*, 2008, **108**, 494–521.
4 P. W. Voorhees, The theory of Ostwald ripening, *J. Stat. Phys.*, 1985, **38**(1–2), 231–252.
5 J. H. Yao, K. R. Elder, H. Guo and M. Grant, Theory and simulation of Ostwald riping, *Phys. Rev.*, 1993, **47**, 14110–14125.
6 S. R. Emory, W. E. Haskins and S. Nie, Direct observation of size-dependent optical enhancement in single metal nanoparticles, *J. Am. Chem. Soc.*, 1998, **120**, 8009–8010.
7 M. Futamata, Y. Maruyama and M. Ishikawa, Microscopic morphology and SERS activity of Ag colloidal particles, *Vib. Spectrosc.*, 2002, **30**, 17–23.
8 J. Tang, P. Photopoulos, A. Tserepi and D. Tsoukalas, Two-dimensional nanoparticle self-assembly using plasma-induced Ostwald ripening, *Nanotechnology*, 2011, **22**, 235306.
9 S. Kim, Y. Han, B. Lee and J. Lee, One-pot fabrication of various silver nanostructures on substrates using electron beam irradiation, *Nanotechnology*, 2010, **21**, 075302.
10 J. Tang, Z. Li, Q. Xia and R. Williams, Fractal structure formation from Ag nanoparticle films on insulating substrates, *Langmuir*, 2009, **25**, 7222–7225.
11 S. Roark, D. Semin, A. Lo, R. Skodje and K. Rowlen, Solvent-induced morphology changes in thin silver films, *Anal. Chim. Acta*, 1995, **307**, 341–353.
12 H. Peng, T. Krauss and B. Miller, Aging induced Ag nanoparticle rearrangement under ambient atmosphere and consequences for nanoparticle-enhanced DNA biosensing, *Anal. Chem.*, 2010, **82**, 8664–8670.
13 P. Redmond, A. Hallock and L. Brus, Electrochemical Ostwald ripening of colloidal Ag particles on conductive substrates, *Nano Lett.*, 2005, **5**, 131–135.
14 S. Gentry, S. Kendra and M. Bezpalko, Ostwald ripening in metallic nanoparticles: stochastic kinetics, *J. Phys. Chem. C*, 2011, **115**, 12736–12741.
15 F. Demoisson, M. Raes, H. Terryn, J. Guillot, H. Migeon and F. Reniers, Characterization of gold nanoclusters deposited on HOPG by atmospheric plasma treatment, *Surf. Interface Anal.*, 2008, **40**, 566–570.

16 X. Lai, T. St. Clair and D. Goodman, Oxygen-induced morphological changes of Ag nanoclusters supported on TiO_2(110), *Faraday Discuss.*, 1999, **114**, 279–284.
17 X. Lai and D. Goodman, Structure–reactivity correlations for oxide-supported metal catalysts: new perspectives from STM, *J. Mol. Catal. A: Chem.*, 2000, **162**, 33–50.
18 T. Hoang, V. La, L. Deriemaeker and R. Finsy, Ostwald ripening of alkane in water emulsions stabilized by polyoxyethylene (20) sorbitan monolaurate, *Langmuir*, 2002, **18**, 1485–1489.
19 M. Vece, D. Grandjean, M. Van Bael, C. Romero, X. Wang, S. Decoster, A. Vantomme and P. Lievens, Hydrogen-induced Ostwald ripening at room temperature in a Pd nanocluster film, *Phys. Rev. Lett.*, 2008, **100**, 236105.
20 Y. Liu, K. Kathan, W. Saad and R. Prud'homme, Ostwald ripening of β-carotene nanoparticles, *Phys. Rev. Lett.*, 2007, **98**, 036102.
21 L. Zhu, G. Lu, S. Mao and J. Chen, Ripening of silver nanoparticles on carbon nanotubes, *Nano*, 2007, **2**, 149–156.
22 G. Upender, R. Sathyavathi, B. Raju, C. Bansal and D. N. Rao, SERS study of molecules on Ag nanocluster films deposited on glass and silicon substrates by cluster deposition method, *J. Mol. Struct.*, 2012, **1012**, 56–61.
23 C. L. Lei, C. C. Wei, M. C. Chen, S. Y. Ou, W. H. Li and K. C. Lee, Enhanced Raman scattering from crystal violet and benzoic acid molecules adsorbed on silver nanocrystals, *Mater. Sci. Eng., B*, 1995, **32**, 39–45.
24 A. Schro1der, J. Fleig, D. Gryaznov, J. Maier and W. Sitte, Quantitative model of electrochemical Ostwald ripening and its application to the time-dependent electrode potential of nanocrystalline metals, *J. Phys. Chem. B*, 2006, **110**, 12274–12280.
25 J. Warreny and B. Murray, Ostwald ripening and coalescence of a binary alloy in two dimensions using a phase-field model, *Modell. Simul. Mater. Sci. Eng.*, 1996, **4**, 215–229.
26 J. Li, Y. Lin and B. Zhao, Spontaneous agglomeration of silver nanoparticles deposited on carbon film surface, *J. Nanopart. Res.*, 2002, **4**, 345–349.